Jurnal Tribologi 19 (2018) 19-38

Jurnal Tribologi
Website : jurnaltribologi.mytribos.org
e-issn: 2289-7232

Initiation of fretting fatigue scar of Ti-6Al-4V alloy dependent on the influence of its surface roughness

Lucian Capitanu [1], Liliana-Laura Badita [2,*], Virgil Florescu [3]

[1] Institute of Solid Mechanics of the Romanian Academy, Bucharest 010141, ROMANIA.
[2] National Institute of Research and Development for Mechatronics & Measurement Technique, Bucharest 021631, ROMANIA.
[3] University of Civil Engineering, Bucharest 050153, ROMANIA.
*Corresponding author: badita_l@yahoo.com

KEYWORD

Ti-6Al-4V alloy
Roughness
Fretting damage
Friction
Wear

ABSTRACT

This paper reports on the experimental studies undertaken to detect the early stage when appears the fretting wear of the Ti-6Al-4V alloy used for the hip prostheses. Wear is a critical aspect for estimating the fretting fatigue. Studies were performed on special shape samples, in order to be able to study the influence of in contact surfaces roughness on the durability to fretting. Fretting pads, with roughness R_a of the contact surface of 0.015 μm and 0.045 μm, and Ti-6Al-4V samples with roughness of 0.045 μm, 0.075 μm and 0.19 μm, were used. Testing periods of 3 seconds, 1 minute and 5 minutes were selected to capture the moment of the fretting scar appearance, long before these initiate the eventual fretting cracking. Simultaneously with the surface fretting wear, the friction coefficient was also measured. From the in-time evolution determinations of the fretting wear, it resulted that, under the experimental conditions used, the minimum wear (V_u = 7.0 × 10^{-6} mm^3) occurs at a certain value of the roughness (0.045 μm) and not at the minimum roughness (0.015 μm). Surprisingly, the minimum friction coefficient (μ = 0.038) does not coincide with the minimum fretting wear (V_u = 7.0 × 10^{-6} mm^3).

Received 26 February 2018; received in revised form 10 May 2018; accepted 7 July 2018.
To cite this article: Capitanu et al. (2018). Initiation of fretting fatigue scar of Ti-6Al-4V alloy dependent on the influence of its surface roughness. Jurnal Tribologi 19, pp.19-38.

1.0 INTRODUCTION

Fretting is a phenomenon that occurs at the interface between two bodies in contact, which are pressed against each other in the presence of cyclic load, which gives rise to a small relative displacement. At the interface there is a complex interaction between wear, corrosion and fatigue. Thus, this phenomenon involves many aspects of contact mechanics, multiaxial fatigue, tribology, and materials science. Directly or indirectly, the damage due to the fretting fatigue is caused by several factors and variables, such as the amplitude of the relative displacement, normal load, tangential and axial loads, material's nature, friction coefficient, cyclic frequency, temperature and the environment. All these factors are interdependent variables that influence this phenomenon.

There are several application domains where this phenomenon occurs, such as aerospace industry, human body implants, automobiles, etc. In the recent years, several studies have focused on understanding this phenomenon, and, of course, finding solutions to prevent and / or avoid it. Designing at fatigue without considering the effect of fretting will certainly lead to premature and unexpected failure in many applications.

Fretting can be classified into two categories: fretting fatigue and fretting wear. Also, corrosion, mentioned in several studies as the third manifestation of the fretting (Buciumeanu et al., 2009), was accepted in the whole area of fretting damage and incorporates the two manifestations of fretting fatigue and fretting wear (Mezlini et al., 2006).

A typical tribo-corrosion action is the materials damage due to mechanical, electrochemical and synergistic effects. These effects are distinct areas of scientific study, but they occur together to cause the wear of a material. A typical example of mechanical experiment includes measurements of tangential load. However, some electrochemical investigations have been performed to help understand the synergistic effects. These synergies have been analyzed to help understand corrosion, both as a mechanical phenomenon and as a mechanical-electrochemical coupled phenomenon (Landolt and Mischler, 2011).

In recent years, several studies have used multiaxial fatigue models to establish correlations with the experimental data of fretting fatigue. The most common multiaxial fatigue models are: Dang Van (DV) – (Kenmeugne et al., 2012, van Lieshout et al., 2017), Smith-Watson-Topper (SWT) – (Ince and Glinka, 2011, Allegretti et al., 2018) and Fatemi and Socie (FS) – (Araujo et al., 2004, Madge et al., 2007, Salerno et al., 2007, Szolwinsky et al., 1998, Lykins et al., 2001, Proudhon et al., 2005, Pellinghelli et al., 2018, Bhatti and Abdel Wahab, 2016).

SWT parameter was used to investigate the behavior of fatigue crack initiation by fretting of the titanium alloy, Ti-6Al-4V (Lykins et al., 2001) and to predict the crack's propagation in a fretting wear case (Fidrici et al. 2005).

Moreover, to match the predicted life with the experimental life, a new factor has been added that takes into account the effect of the residual compression stresses induced by the stricking blow. Araujo and Nowell, 2002, have demonstrated that the use of the SWT and FS approaches to estimate the life of fretting fatigue initiation of Ti-6Al-4V is not appropriate if the calculations are based exclusively on the stress-strain behavior of the surface at extremely tensioned points. This suggested that these methods would not be adequate for assessing the life of fretting fatigue initiation in tests with different geometries, and that the reason for the poor performance of the prediction methodology is the presence of the effects of the high stress gradient. Considering the effect of the stress gradient and combining with a multiaxial fatigue criterion, they proposed two methods of averaging which would give a less conservative prediction of the life of fretting fatigue initiation. The first method is an average of the SWT and FS parameters over a characteristic depth

on the critical plane. The second method is an average of the stresses in a characteristic elementary volume. Both methods of calculating the average produced sensible similarly results.

The fretting problem was also approached as a problem of simple fatigue subjected to a localized stress concentration (Giannakopoulos et al. 2000). This has been done by developing an analytical model for fretting fatigue at a corner of a rounded mandrel in contact with a substrate, and an analogy with the initiation of the fatigue crack at the notch of a tip was made. They analyzed the similarities and differences between the stress concentration factors at the edge of the mandrel-on-flat unexpectedly rounded contact and the tip of a blunt crack. Notch-like methodology provided a direct connection between the life of the fretting fatigue crack initiation of a flat mandrel with rounded corners and the life of the simple fatigue crack initiation of a smooth sample made of the same material. These model predictions showed good concordance with the fretting fatigue experiments on Ti-6Al-4V.

The wear is a critical aspect for estimating the fretting fatigue and can have a major effect on the predicted evolution of the stresses and deterioration parameters (e.g. SWT), and, thereafter, on the predicted fatigue life and the position's failure (Madge et al., 2007). They argued that this fundamental and important effect of fretting fatigue wear cannot be predicted by models that do not include the material's removal effect due to the wear. They performed a finite elements simulation (removed element simulation), which simultaneously combines a fretting wear model (on a modified version of the Archard's wear equation that is used to predict the effect of the material removal due to the wear) and the SWT parameter of fretting fatigue, which includes the effect of the stress peak.

From the various approaches mentioned above, one can conclude that is still missing a more comprehensive analysis of the fretting fatigue phenomena. The data currently available on different materials and test conditions are insufficient to allow taking a decision on a suitable model.

The models chosen for examination are two models of fatigue based on deformation. The first approach is the Smith-Watson-Topper model, and the second approach is Morrow's model. The first model is already used in fretting fatigue, while the latter was first tested for fretting fatigue situations by Buciumeanu et al., 2009. In both models, the effects of average stress are included. Morrow's model was modified to introduce the local stresses involved in the fretting fatigue process (normal, tangential and axial). Moreover, a new parameter, which is a stress concentration factor, K_t, which includes the effect of the affected area, called in this work, the "effect of the fretting scar", has been introduced in both models.

In accordance with the direction of relative movement under a ball-on-flat (BOF) contact configuration, four basic fretting modes can be distinguished, namely: tangential, radial, rotational and torsional fretting. Rotational fretting, representing the relative movement induced by the micro-amplitude rotation that takes place in the pair of contacts with tightly fixing in the alternative loading medium, results in wear of the contact surface that exist in many mechanical and biomedical equipment and instruments. Researches on rotating fretting (rotation and torsion) modes wear under the BOF contact configuration were performed by Zheng et al., 2011, Yang et al., 2013, Zhou et al., 2017, Shen et al., 2015, Shen et al., 2016, Luo et al., 2016, Done et al., 2017, Shen et al., 2013.

However, the contra-pair contact configurations, in which the fretting damage occurs in practice, are often not BOF contacts, but also other contact configurations like concave-to-concave, curve-to-curve. For example, for the ball and socket joints in the modern industry, double rotating fretting wear (combined with rotating and torsional fretting) has been performed in a curve-to-

curve contact configuration. According to the modern tribological theory, the behaviors of contact stress, of contact stiffness and of contact residues are quite different under different contact configurations. The contact configuration plays a very important role in the fretting wear. In order to understand the rotating fretting mechanisms in the different contact configurations, rotating fretting tests with ball-on-concave (BOC) and ball-on-flat (BOF) contacts were performed at the same maximum contact stress and, respectively, normal loads.

Many research works have been done on the wear mechanisms by fretting and fatigue. Various fretting regimes have been identified and fretting maps or fretting journals have been successfully used to study the fretting behavior of different materials. It has been achieved the understanding of some basic mechanisms of fretting, allowing the development of various possible palliatives. However, to date, there has been no general agreement on the mechanisms and modeling of fretting. For example, the mechanical, chemical, tribological and electrical processes between the two contact surfaces during the fretting were not fully understood, because the most models and wear theories are based on the observation of deterioration by the fretting wear. The direct or in situ observation of the fretting wear process implies the procurance of time-dependent changes and casts lighter on the actual fretting mechanisms (Fu, Y.Q., et al., 2000).

Fretting in a total hip prosthesis results from the destruction of the passive oxide layer from the metal, thus leading to increased corrosion and to the residues generation, such as polymer and/ or metal oxides particles, resulting in serious dysfunctions of the hip joint (Kim K., et al., 2013, Batchelor et al., 1992, Geringer et al., 2005, Geringer and Macdonald, 2012, Garcia and Grandt, 2005, Magaziner et al., 2008). The cyclic loading due to the daily human walking, and the differences between the mechanical properties of the femoral stem and bone cement give rise to the separation of the two materials. This unsoldering leads to secondary effects, such as degradation and cracking of cement. Residues, including metal oxides and ions, invade bone tissues through cracks and finally induce inflammation in the bone tissues. This study presents the experimental and theoretical research on the fretting behavior of the Ti-6Al-4V alloy samples used for the manufacture of total hip prostheses.

2.0 EXPERIMENTAL PROCEDURE

2.1 Experimental assembly for testing

The fretting tests were performed on a universal servo-hydraulic testing machine, MTS Bionix, Figure 1. The testing machine allowed application of a 600 kN load under static conditions and 500 kN for fatigue loading. The maximum cyclic loading frequency of the machine is 50 Hz. The equipment operates at ambient temperature in the laboratory environment but can also be used at low and high temperatures and with other environments. To perform fretting fatigue tests, on the machine was a special fretting device that has two load cells that allow (prior to testing) application of normal and tangential contact loads (during the test) and their recording/ measurement. A 1000 N loading cell is used to set and measure the pre-tangential/ tangential load and a 2500 N loading cell to set/ measure the normal load. The load is applied by two pads, which are pressed perpendicularly on the flat faces of the sample by a pair of compression springs, which are loaded with adjustable screws. Also, two vertical compression springs, which action on the pad, are used to apply the pre-tangential load (to avoid the pad's movement).

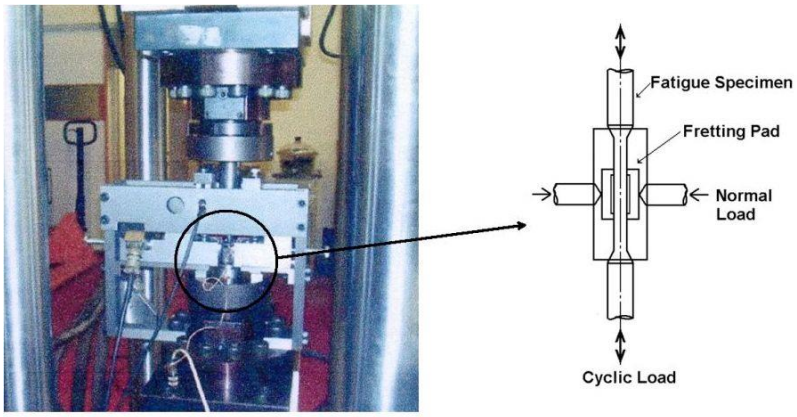

Figure 1: MTS Bionix servo-hydraulic dynamic testing machine.

"Bridge" type fretting pads were used, which have as main advantage the simplicity with which a normal fatigue specimen can be used, both at bending and at cyclic traction. The bridges are simply fixed to the sides of the specimen by a ring or a similar arrangement and the cyclic deformation of the specimen causes a relative movement between the bridge legs and the specimen.

Unfortunately, there are several difficulties with such a simple arrangement. The contact conditions at the pad legs are difficult to characterize, especially if bending occurs in the bridge itself. In addition, the conditions of each leg will not be the same, and it is possible that one leg to slide before the other, even under symmetrical nominal conditions. This means that the sliding regime during the experiment is often unknown. Therefore, the pads were made of RUL1 bearing steel, hardened and polished to a roughness R_a of 0.15 μm. The tangential load varies depending on the axial load of the machine. Due to the system's symmetry, loads are measured only in one part. The axial cyclic load applied to the sample was monitored with the machine's loading cell.

2.2 The geometry of the sample and the pad

Fretting fatigue experiments were performed using the geometries of sample and pad, which are shown in Figure 2, and Figure 3 shows the scheme of the sample-pad contact test configuration. The specimen (Figure 2) has a special shape, with two flat opposite faces (A), milled, rectified and polished in the middle of the sample. In this situation, the two contact areas on the flat sides of the sample were generated. In the middle of these areas, holes with diameter of 10.1 mm and depth of 2.5 mm were drilled. Fretting samples were introduced into these places. This was done in order to study the influence of in contact surfaces roughness to the durability at fretting. Several pads and fretting samples were produced, which had been finished with roughness Ra = 0.015 μm. The spherical head of the pads had a roughness of 0.05 μm. Prior to testing, the samples and pads surfaces were ultrasonically cleaned in alcohol. Figure 3 schematically shows the configuration of the sample-pad contact testing in the fretting fatigue tests.

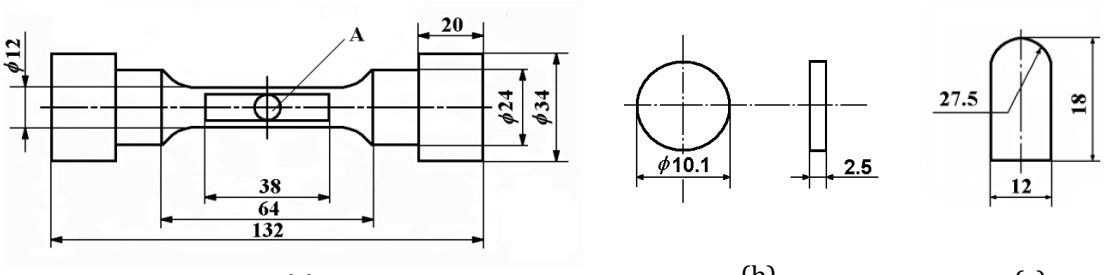

(a) (b) (c)

Figure 2: Geometry of the specimen (a), sample (b) and fretting test pad (c)

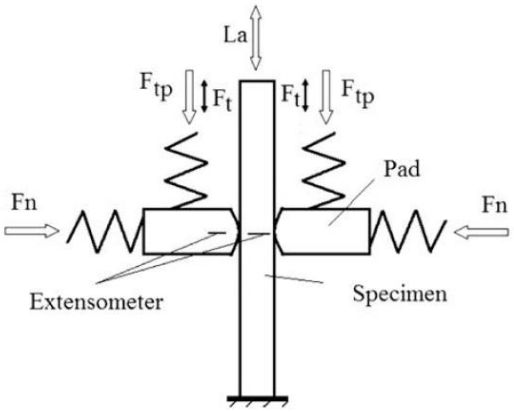

Figure 3: Scheme of the test configuration of the sample-pad contact: Fn - normal loading of the pad; Ftp - tangential pre-loading of the pad; Ft - tangential loading of the pad and La - axial load of the machine.

2.3 Experimental procedure

Under static conditions, the compressive stresses due to contact point, $p_{\max}$ and p_{med} (maximum and average contact pressure) are given by:

$$p_{max}^3 = 1.5\, PE^2 \,/\, \pi r^2 (1 - \mu^2)^2 \tag{1}$$

$$p_{med} = \frac{P}{\pi a^2} \tag{2}$$

While the radius a of the circular contact surface is:

$$a^3 = 1.5(1-\mu^2)P\frac{r}{E} \tag{3}$$

Where P is the load; a is radius of the contact surface and r is the radius of the spherical head of the pad and E is the elastic modulus (Williams and Dwyer-Joyce).

For coupling components made of steel, the values of the previous equations become:

$$p_{max} \approx 5800\, \sqrt[3]{P} \tag{4}$$

$$p_{med} \approx 1700\, \sqrt[3]{P} \tag{5}$$

$$a \approx 0.09 \sqrt[3]{P} \tag{6}$$

Particular attention was given to the finishing of the specimens' friction surfaces. The state of the surface, being defined by topography, microstructure of the superficial layer and the oxidation state, has a major contribution to the wear process. Due to the complexity of surface creation through an abrasion process, the safest way to ensure a consequent reproducible surface is strictly by adhering to all stages of the finishing process.

The following stages have been established: shape transformation, finishing transformation, thermal treatment, rectification, fine adjustment and ultimately super-finishing of the work surface. While in all the stages, until the fine final adjustment, traditional manufacturing techniques are used, it is worth mentioning that the overall intensity of the process is deliberately maintained at a low level to protect the superficial structure of the material. The super-finishing stage uses the metallographic polishing techniques and includes: wet polishing with abrasive paper of 32 μm and 17 μm granulation, polishing with diamond paste of 6 μm and 1 μm granulation, and finally wet polishing using alumina suspension having a granulation of 2000 Å. The surfaces are then cleaned with alcohol and distilled water and then are dried. The storage of the finished samples is done in sealed containers on a layer of silica gel.

After the super-finishing stage, four different roughness values were obtained for Ti-6Al-4V samples surfaces: R_a = 0.015 μm, R_a = 0.045 μm, R_a = 0.075 μm and R_a = 0.19 μm. Surfaces roughness was determined using a profilometer with parametric transducer and graphical recording, Perth-O-Meter. The tool allows not only the recording of surface profiles, but also the determination of the R_a and *r.m.s* values, defined as (Bhushan, 2001):

$$R_a = \frac{1}{l}\int_0^l |y| dx \tag{7}$$

$$r.m.s = \left(\frac{1}{l}\int_0^l y^2 dx\right)^{1/2} \tag{8}$$

The tests mainly followed the evolution of fretting scar according to the normal load applied under different roughness conditions of the surface and normal loading, but at constant tangential loading. Experimental tests were performed under lubrication conditions with SBF (simulated body fluid) from Hyclone Inc., USA, which has a composition close to that of the human serum.

3.0 RESULTS AND DISCUSSION

Fretting fatigue tests were performed at a stress ratio R = 0.1 where $R = F_n / F_t$. All tests were performed at ambient temperature, in the laboratory environment, as well as at a cyclic frequency of 4 Hz. The profiles and microphotographs of the initial surface topography with initial roughness R_a = 0.015 μm (A1-A2), R_a = 0.045 μm (A3-A4), R_a = 0.075 μm (A5-A6) and R_a = 0.19 μm (A7-A8) are illustrated in Figure 4.

In order to properly view the wear of the fixed surface, depending on the roughness of the coupling, the following solution was used: the coupling asperities were concentrated on one of the surfaces, especially on the mobile one. Fixed surface has always had the minimum achievable

roughness, i.e. approximately $R_a \approx 0.015$ μm. As is well known, the composite roughness of the coupling, expressed by standard deviations, σ, is:

$$\sigma^2 = {\sigma_1}^2 + {\sigma_2}^2 \quad (9)$$

Where σ_1, σ_2 represent the standard deviations of the two surfaces.

If one of the surfaces has a much smaller roughness, i.e. $\sigma_1 << \sigma_2$, then $\sigma \approx \sigma_1$. Thus, it is possible to study the influence of roughness on wear, even by changing the roughness of a single surface. In these conditions and under a load P = 30 N, the relative velocity u = 1.74 m/s and at the temperature θ = 50 ^{0}C of the lubricant volume, the evolution of the surface wear was developed in function of time for the following roughness of the mobile surface: R_a = 0.015 μm; R_a = 0.045 μm; R_a= 0.075 μm and R_a = 0.19 μm.

3.1 Evolution of the contact surface state in fretting conditions

The consequence of fretting is the fretting scar that forms in the area of the pad-sample contact and which can evolve by initiating the fretting crack until the sample breaks over time. The initiation phase takes almost 80% of the coupling's runtime. In Figure 5, some fretting wear scars obtained under the above-mentioned conditions (at time t = 5 min) are shown selectively to estimate the reproducibility of the results.

The scar volume for the three experimental determinations is: 1057 specimen: V = 8.50 x 10^{-5} mm^3; 1058 specimen: V = 6.11 x 10^{-5} mm^3; 1059 specimen: V = 4.00 x 10^{-5} mm^3, resulting an average volume $\overline{V}$ = 6.2 x 10^{-5} mm^3. For wear measurements, a deviation of 25% is completely satisfactory.

Figure 6 shows the evolution of the wear depending on time, for the roughness of the pad R_a = 0.045 μm. Trial times of 3 seconds, 30 seconds, 1 minute and 5 minutes were selected, each performed with another coupling. For the roughness R_a = 0.045 μm, the evolution of wear versus time was determined with the same pad, the total fretting time on the scar being divided in intervals of 1, 5, 3 or 10 minutes. This solution was chosen to also monitor the change of the pad surface state. Figure 6 shows that, except for the first 5 minutes, the wear remains at the same level. In Figure 7 is shown the transversal profile and the image of the fretting wear scar for the sample with R_a = 0.045 μm, t = 5 min (sample 703); R_a = 0.045 μm, t = 5 min, but with the pad from the previous determination (total operating time t = 10 min, sample 704); R_a = 0.045 μm, t = 5 min, with the pad from the previous determination (total operating time t = 20 min, sample 705).

The evolution of fretting wear depending on time for different roughness is presented in the double-logarithmic diagram in Figure 8. By increasing the operating time from 5 minutes to 30 minutes, the wear increases by only about 10%. It is worth noting the rapid reduction of the wear velocity over time, excepting the surface with roughness R_a = 0.045 μm. In the first 3 seconds, between 25% and 50% of the wear occurs in 30 minutes. This evolution of wear is explained by the surfaces running, which leads to a change in the lubrication regime. Note that the amount of wear on the plate is caused by the initial wear (in the first few seconds of operation). This observation allows the use of the wear value at t = 5 min as a representative quantity for the existing operating conditions. During this operation period, the values scattering is small. In the case of surfaces with R_a = 0.045 μm, the wear is so low that during the entire period used, the lubrication conditions remain roughly unchanged.

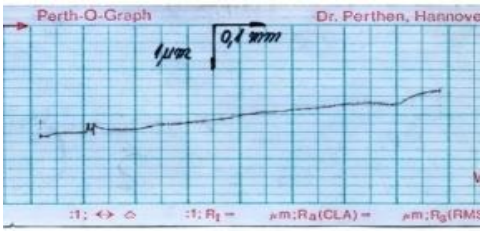

A1

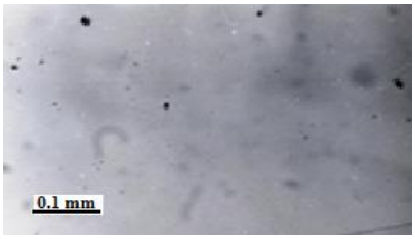

A2

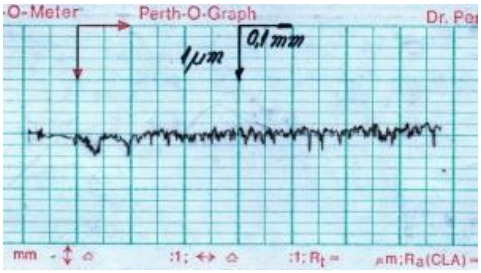

A3

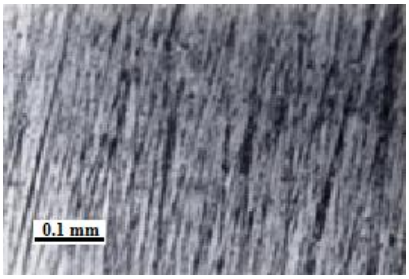

A4

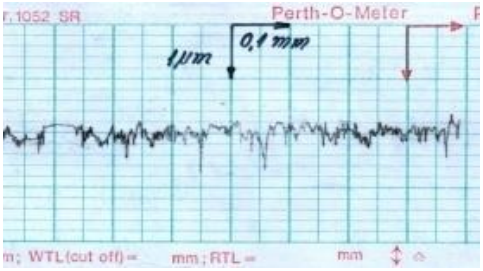

A5

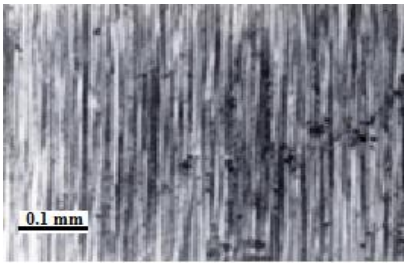

A6

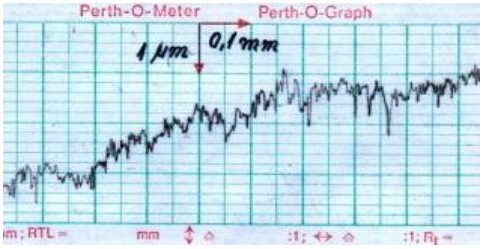

A7

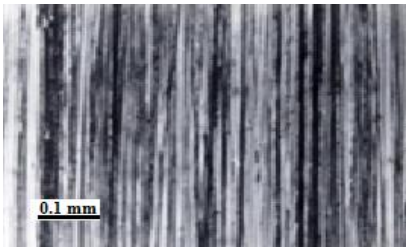

A8

Figure 4: Profiles and microphotographs of the initial surface topography with roughness R_a = 0.015 µm (A1-A2), R_a = 0.045 µm (A3-A4), R_a = 0.075 µm (A5-A6) and R_a = 0.19 µm (A7-A8).

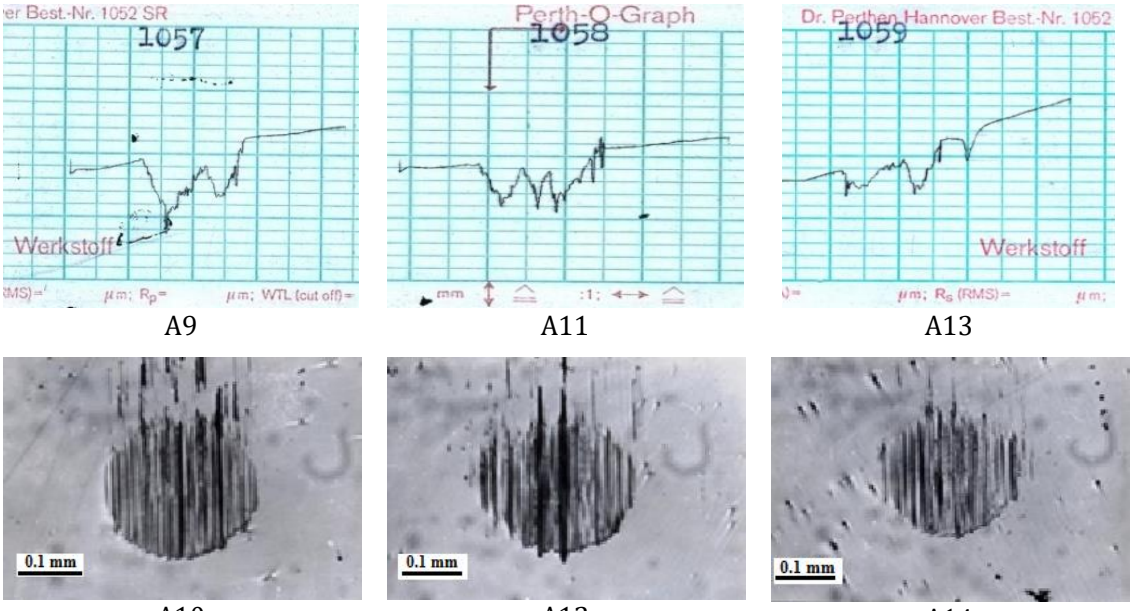

A9 A11 A13

A10 A12 A14

Figure 5: Central transversal profile and image of fretting wear scar. Ra = 0.015 µm, t = 5 min.

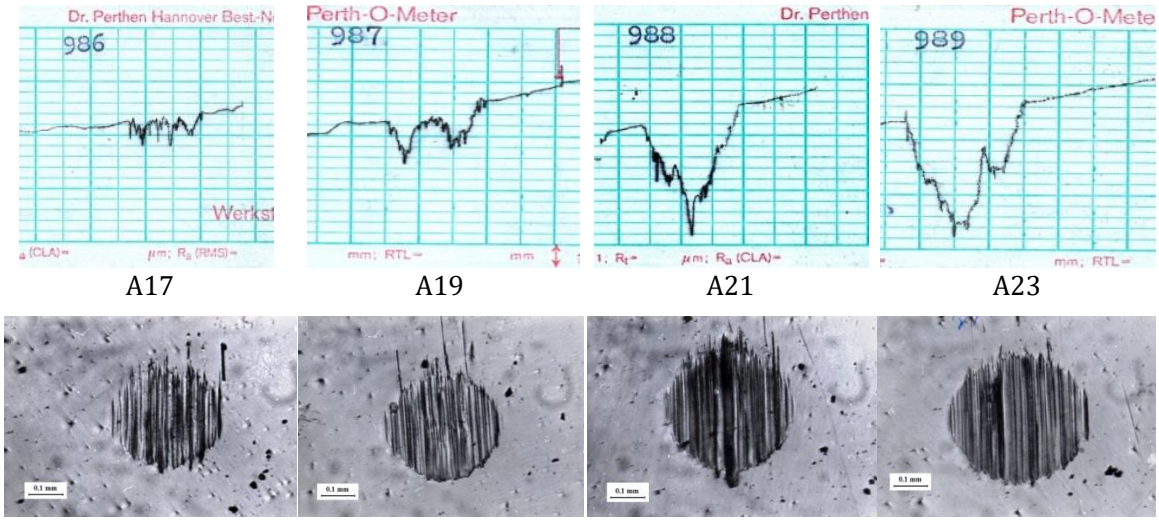

A17 A19 A21 A23

A18 A20 A22 A24

Figure 6: Central transversal profile and image of fretting wear scar Ra = 0.045 µm, t = 5 min.

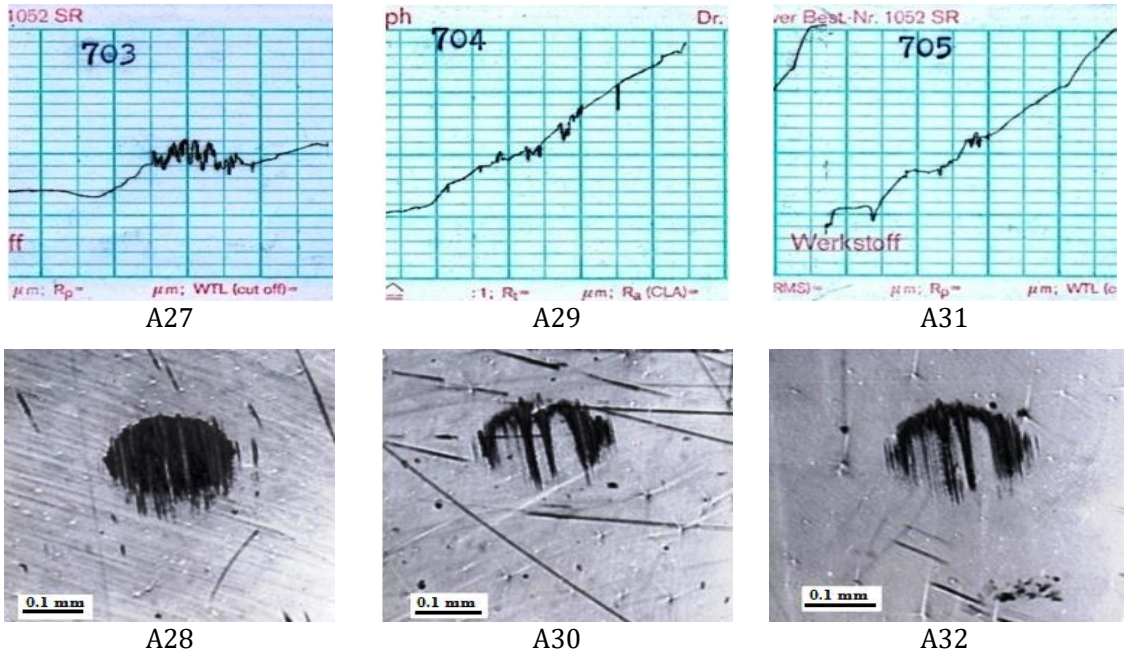

Figure 7: Profile and image of the fretting wear scar for samples with R_a = 0.045 µm, t = 5 min. (sample 703); R_a = 0.045 µm, t = 5 min., with the pad from the previous determination – total operating time t = 10 min. (sample 704); R_a = 0.045 µm, t = 5 min., with the pad from the previous determination – total operating time t = 20 min. (sample 705).

The evolution of the fretting wear function of time, for roughness R_a = 0.075 µm (samples 829, 830 and 832) is shown in Figure 9. Different roughness used have caused not only a difference between the amount of wear volume of the scar, but also of the wear scar appearance (the type of wear). In the case of the surfaces with R_a = 0.015 µm, R_a = 0.075 µm (t = 3 s) and R_a = 0.19 µm (t = 3 s), the wear is of adhesive type (metallic shape with pronounced scratches). In the case of surfaces with R_a = 0.045 µm, the fretting wear type is predominantly oxidative. While the fretting wear velocity is reduced due to surface conformation, the surfaces with R_a = 0.075 µm and R_a = 0.19 µm also undergo in oxidative wear regime.

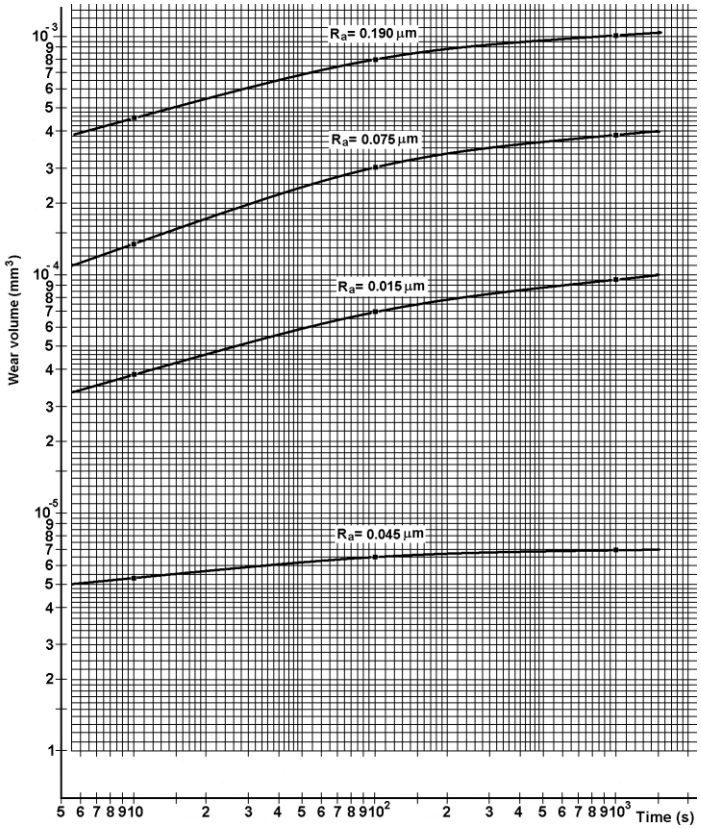

Figure 8: Evolution of wear versus time, for different roughness R_a.

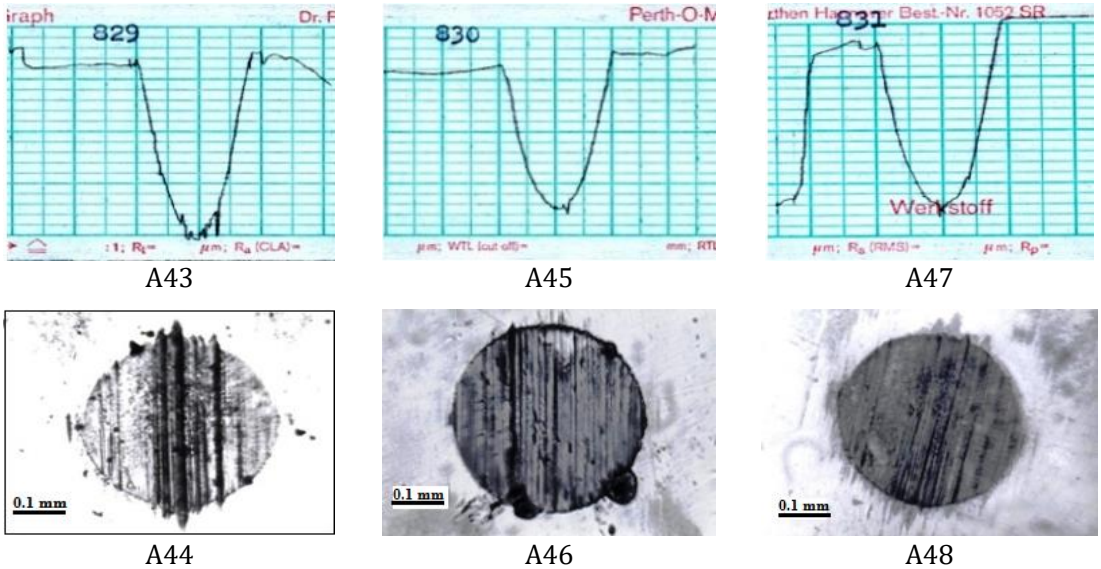

A43 A45 A47

A44 A46 A48

Figure 9: Evolution of the fretting wear function of time, for R_a = 0.075 µm (samples 829, 830, 832).

The evolution of the fretting wear function of time, for roughness R_a = 0.19 μm (samples 835, 849, 836, 837 and 850) is shown in Figure 10.

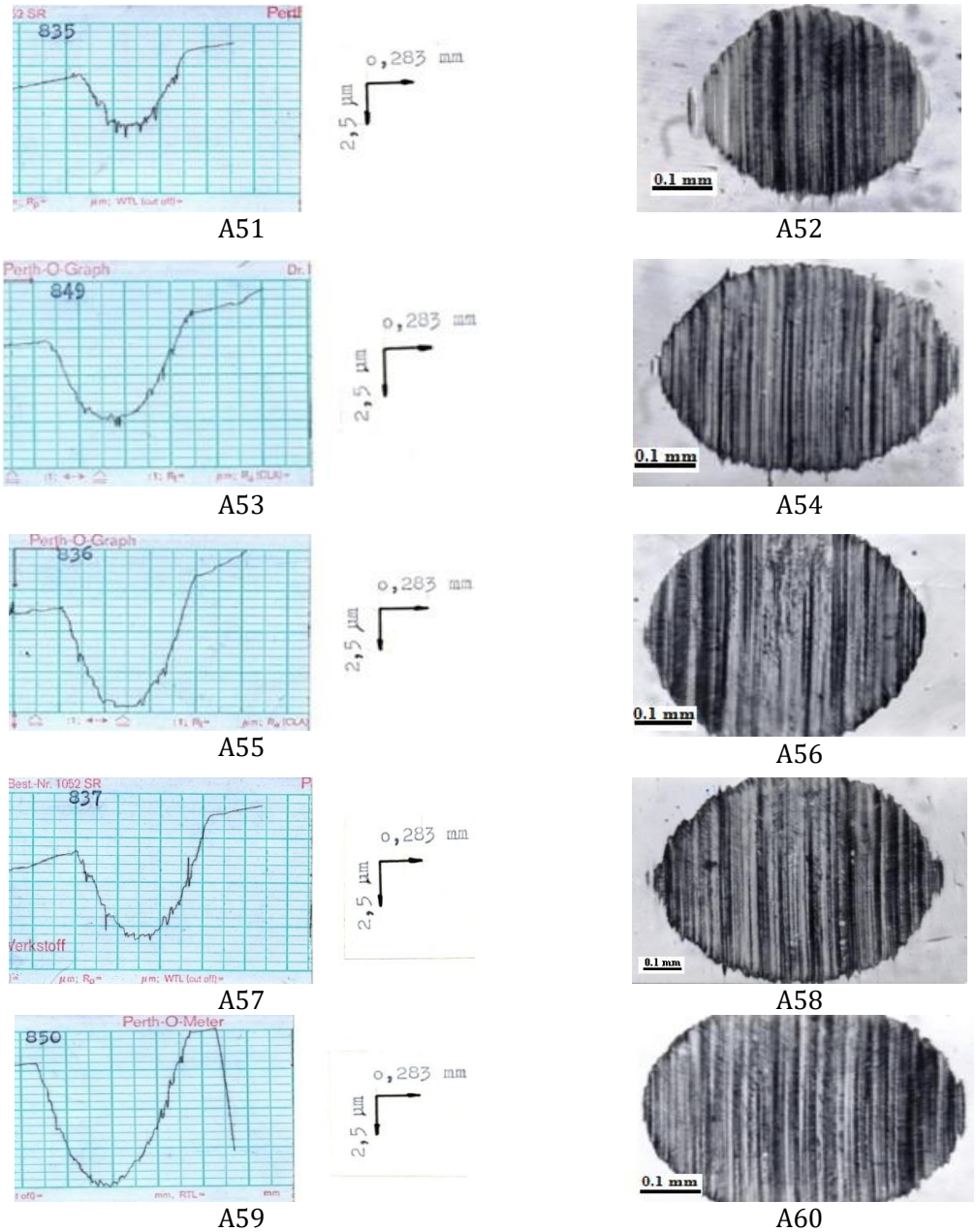

Figure 10: Evolution of the fretting wear function of time, for roughness R_a = 0.19 μm (samples 835, 849, 836, 837 and 850).

For the roughness R_a = 0.015 μm, R_a = 0.075 μm and R_a = 0.19 μm, the results obtained for the volume of the worn material are in accordance with the contact deformation, determined by the parameter of the lubricant film h_{min} / σ. For surfaces with roughness R_a = 0.045 μm, an influence of the running-in was observed. After the first 5 minutes of operation, the entire contact surface is covered with oxide. The scar obtained after another 5 minutes, with the same pad, has a special shape, the oxidative wear area is limited to half of the loaded surface (samples A52 and A54).

Figure 11 shows the central profile and the image of the fretting wear scar R_a = 0.19 μm, t = 30 min, sample 997 (new pad). Next, Figure 12 shows the effect of the running-in on the fretting wear behaviour of the surface with R_a = 0.19 μm, with the same pad as in the previous test, compared to Figure 13, that shows the effect of the running-in on the wear behavior of the surface with roughness R_a = 0.045 μm, using a new pad. In the experimental conditions of Figures 11 and 12, it is clearly observed the start of the fretting scars elongation in the sliding direction (from top to bottom A61 / A62 and A63 / A64) and the typical W-shape of the transversal profile of the scar, noted in many of the papers published in the field (Batchelor et al., 1992, Geringer et al., 2005, Geringer and Macdonald, 2012, Garcia and Grandt, 2005, Magaziner et al., 2008).

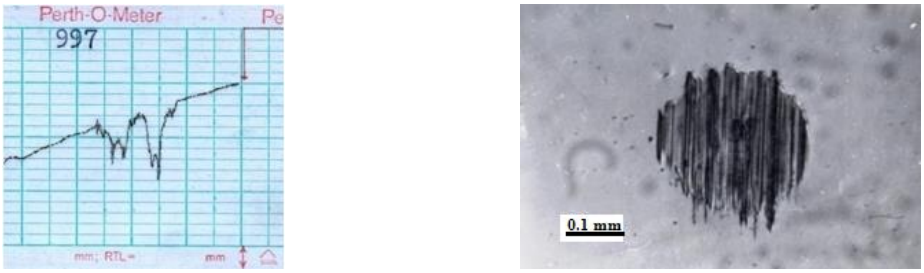

A61 A62

Figure 11: Central transversal profile and image of wear scar. R_a = 0.19 μm, t = 30 min., sample 997, (new pad).

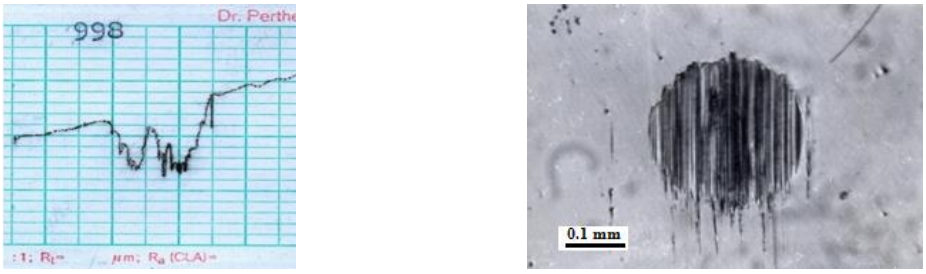

A63 A64

Figure 12: The effect of running-in on the fretting wear behaviour of the surface with R_a = 0.19 μm, t = 5 min, sample 998. The pad from previous determination was used.

In the case of super-finished surfaces with R_a = 0.015 μm no favorable influence of the running-in is observed. For surfaces with roughness of R_a = 0.045 μm, a favorable influence of the running-in was observed (Figure 13). After the first 5 minutes of operation, it was observed that the entire contact surface was coated with oxide. The scar obtained after another 5 minutes, with the same pad, has a special shape, the oxidation wear area being limited to half of the loaded surface (sample 1002) - Figure 13.

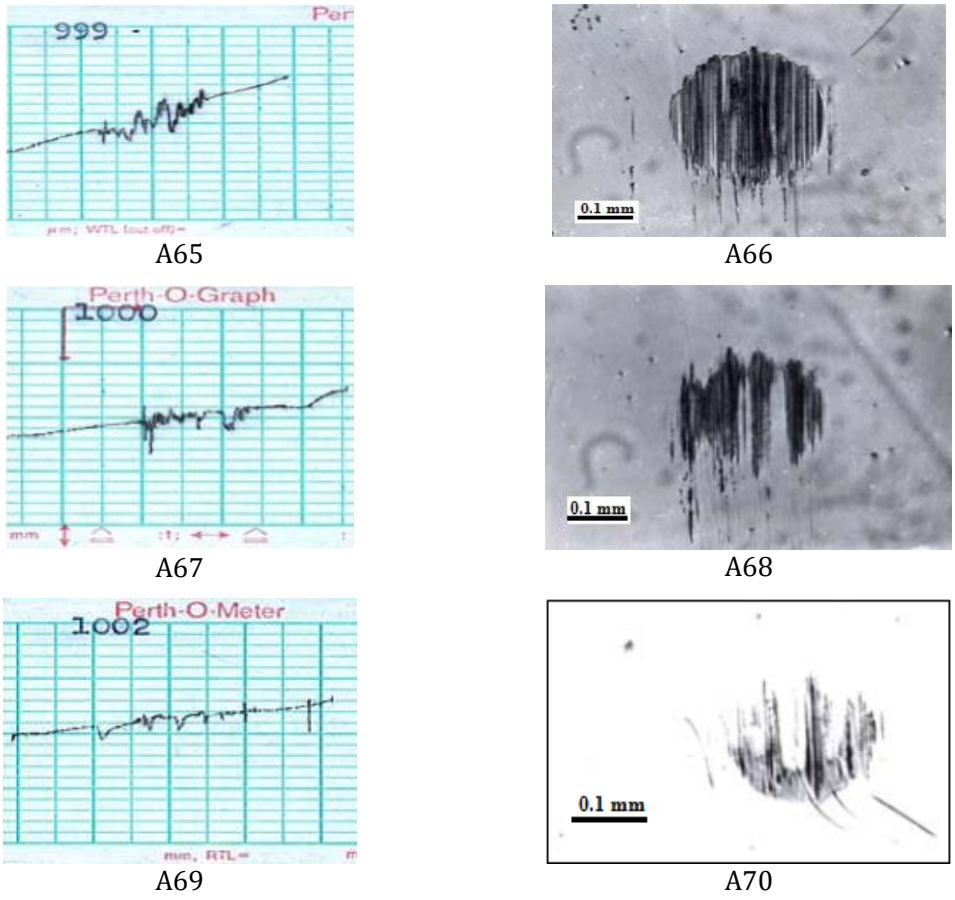

Figure 13: The effect of the running-in on the fretting wear behaviour of the surface with R_a = 0.045 μm, t = 5 min, samples 999 (with new pad), 1000 and 1002 (with the pad from the previous determination).

3.2 Influence of the initial roughness on the fretting wear and friction coefficient

The minimum value of the surface wear must coincide with the minimum value of the surface roughness. Many wear measurements were performed with four roughness: R_a = 0.015 μm; R_a = 0.045 μm; R_a = 0.075 μm and R_a = 0.19 μm. The average values of the volume of fretting worn material for the four roughness are:

$$R_a = 0.015\ \mu m \rightarrow V_u = 7.0 \times 10^{-5}\ mm^3 \rightarrow \mu = 0.038;$$
$$R_a = 0.045\ \mu m \rightarrow V_u = 7.0 \times 10^{-6}\ mm^3 \rightarrow \mu = 0.050;$$
$$R_a = 0.075\ \mu m \rightarrow V_u = 3.7 \times 10^{-5}\ mm^3 \rightarrow \mu = 0.038;$$
$$R_a = 0.190\ \mu m \rightarrow V_u = 1.0 \times 10^{-3}\ mm^3 \rightarrow \mu = 0.078.$$

Simultaneously with the production of fretting wear scars on the surface of the Ti-6Al-4V alloy samples, the coefficient of friction was also measured. The effect of the running-in on the fretting

wear behavior of the surface was also analyzed. This was done by using the same pad for several successive tests.

In Figure 14 are shown representative images of the running-in effect on the fretting wear behavior of the surface with the pad from the previous determination, for three of the four roughness (samples 1077, 1065 and 1067). The existence of an optimal roughness can be explained either by an effect on the lubricant film or by a change in the mechanical properties of the surface. In this case, at the optimum roughness, the reduction of the h / σ ratio is compensated by increasing the wear resistance of the surfaces. In the experimental conditions used, the fretting contact between the pad and the sample was a point contact, which produced a fretting wear scar that evolved rapidly even during the short time considered (maximum 30 minutes).

The influence of the sample and pad roughness on the initiation and evolution of the fretting wear scar was studied. The geometry of the test configuration allowed the investigation of finished surfaces at roughness R_a = 0.015 μm, R_a = 0.045 μm, R_a = 0.075 μm and R_a = 0.19 μm. From the determinations of fretting wear evolution in time under the experimental conditions used (short testing time), it was found that in the case of the shortest experiment (5 minutes) the fretting wear scar is visible. The profiles and microphotographs of the initial surfaces topography studied and of those resulted after short fretting contact periods were recorded and analyzed. Simultaneously the friction coefficient was measured.

The recording of fretting scars allowed calculation of the volume of worn material by fretting and correlation with the value of the friction coefficient recorded during each test. It has been found that there is a minimum of the wear curve resulted for roughness R_a = 0.045 μm. After 3 seconds, in the case of surfaces with R_a = 0.015 μm, R_a = 0.075 μm and R_a = 0.19 μm (t = 3 s), the fretting wear is of adhesive type (metallic shape with pronounced scratches). In the case of surfaces with R_a = 0.045 μm, the type of fretting wear is predominantly oxidative.

During the running-in, the fretting wear velocity is reduced as a result of the surface conformation, and surfaces with R_a = 0.075 μm and R_a = 0.19 μm are undergoing in oxidative wear regime. It has been observed that by increasing the operating time from 5 minutes to 30 minutes, the wear increases only with about 10%. It is worth noting the rapid reduction of the wear velocity over time, excepting the surface with roughness R_a = 0.045 μm, where in the first 3 seconds, between 25% and 50% of the wear occurs in 30 minutes. At surfaces with roughness R_a = 0.045 μm, a significant influence of the running-in was observed. After the first 5 minutes of operation, the entire contact surface is covered with oxide. The scar obtained after another 5 minutes, with the same pad, has a special shape, the oxidative wear area being limited to half of the loaded surface.

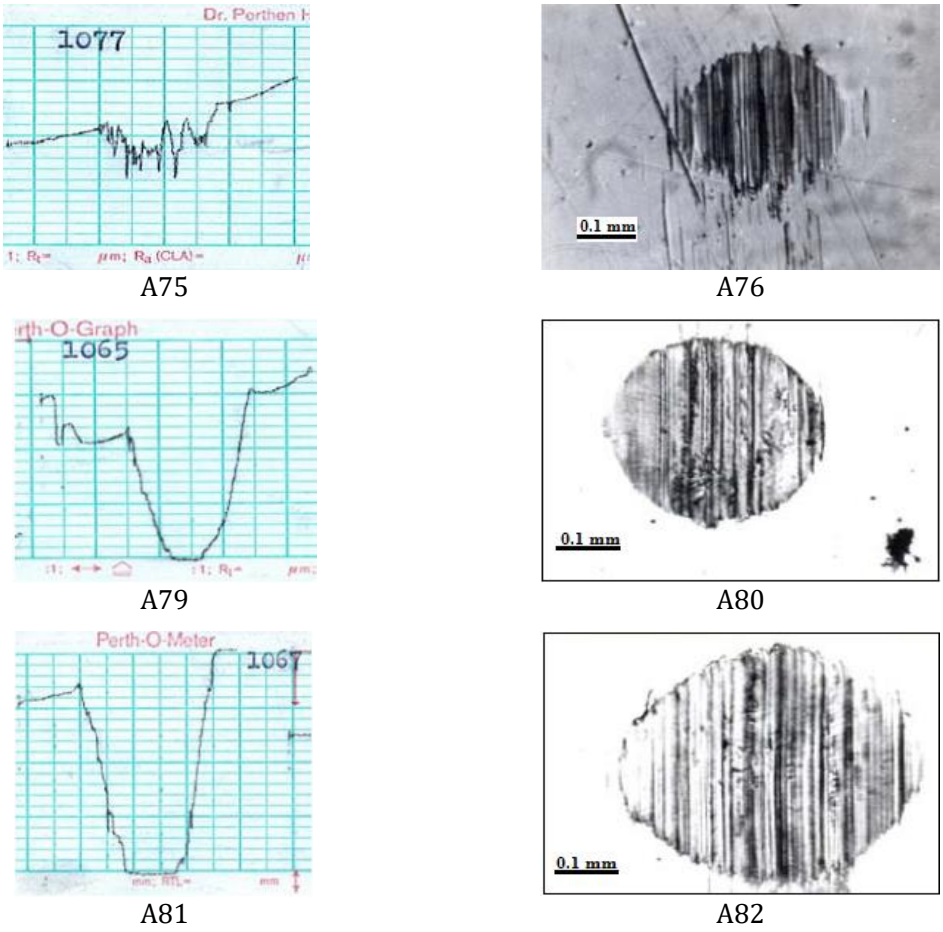

Figure 14: Effect of the running-in on the fretting wear behaviour of the surface with R_a = 0.19 µm, t = 5 min, samples 1077, 1065 and 1067 (with the pad from the previous determination).

4.0 CONCLUSIONS

(a) Under the experimental conditions used, the initiation of the fretting scar occurs within the first 5 minutes of the couple operation.

(b) A double-logarithmic evolution of fretting wear function of time was determined for different roughness analyzed. The used roughness caused not only a difference in the value of the scratch scar removal volume but also the appearance of wear scar (type of wear). Used roughness have caused not only a difference between the values of the worn volume of the fretting scar, but also of the wear scar appearance (type of wear).

(c) In the experimental condition Ra = 0.015 µm, t = 5 min and Ra = 0.19 µm, t = 30 min it is clearly observed the start of the fretting scars elongation in the sliding direction, as well as the typical W-shape of the transversal profile of the scar, noted in many of the papers published in the field.

(d) It was found the existence of a minimum of the resulting wear curve for roughness Ra = 0.045 μm, but which surprisingly does not coincide with the minimum friction coefficient.
(e) A mathematical relationship between the friction coefficient and wear cannot be established.

ACKNOWLEDGEMENT

The authors gratefully acknowledge the financial and logistic support of Department of Technical Sciences of the Romanian Academy.

REFERENCES

Allegretti, D., Berti, F., Migliavacca, F., Pennati, G., & Petrini, L. (2018). Fatigue assessment of nickel-titanium peripheral stents: Comparison of multi-axial fatigue models. Shape Memory and Superelasticity, 4, 1-11.

Araujo, J. A. & Nowell, D. (2002). The effect of rapidly varying contact stress fields on fretting fatigue. International Journal of Fatigue, 24, 763–775.

Araujo, J. A., Nowell, D. & Vivacqua, R. C. (2004). The use of multiaxial fatigue models to predict fretting fatigue life of components subjected to different contact stress fields. Fatigue& Fracture of Engineering Materials and Structures, 27, 967–978.

Batchelor, A. W., Stachowiak, G. W., & Stachowiak, G. B. (1992). Control of fretting friction and wear of roping wire by laser surface alloying and physical vapour deposition coatings. Wear, 152, 127-150.

Bhatti, N. A., & Abdel Wahab, M. (2016). A review on fretting fatigue crack initiation criteria. International Journal of Fracture Fatigue and Wear, 4, 78-85.

Bhushan, B. (2001). Surface roughness analysis and measurement techniques. In Modern tribology handbook, ed. Bharat Bhushan, volume one – Principles of tribology. CRC Press LLC, chapter 2

Buciumeanu, M., Crudu, I., Palaghian, L., Miranda, A. S., & Silva, F. S. (2009). Influence of wear damage on the fretting fatigue life prediction of an Al7175 alloy. International Journal of Fatigue, 31, 1278–1285.

Done, V., Kesavan, D., Huffman, M., & Nelias, D. (2017). Accelerated fretting wear tests for contacts exposed to atmosphere. Tribology Letters, 65, 153.

Fidrici, V., Fouvry, S., Kapsa, P., & Perruchaut, P. (2005). Prediction of cracking in Ti-6Al-4V alloy under fretting-wear: use of the SWT criterion. Wear, 259, 300–308.

Fu, Y. Q., Wei, J., & Batchelor, A. W. (2000). Some considerations on the mitigation of fretting damage by the application of surface-modification technologies. Journal of Materials Processing Technology, 99, 231-245.

Garcia, D. B., & Grandt, A. F. Jr. (2005). Fractographic investigation of fretting fatigue cracks in Ti–6Al–4V. Engineering Failure Analysis, 12, 537–548.

Geringer, J., & Macdonald, D. D. (2012). Modeling fretting-corrosion wear of 316L SS against poly(methyl methacrylate) with the point defect model: Fundamental theory, assessment, and outlook. Electrochimica Acta, 79, 17– 30.

Geringer, J., Forest, B., & Combrade, P. (2005). Fretting-corrosion of materials used as orthopaedic implants. Wear, 259, 943–951.

Giannakopoulos, A. E, Lindley, T. C, Suresh, S., & Chenut C. (2000). Similarities of stress concentrations in contact at round punches and fatigue at notches: implications to fretting fatigue crack initiation. Fatigue & Fracture of Engineering Materials & Structures, 23, 561–571.

Ince, A., & Glinka, G. (2011). A modification of Morrow and Smith-Watson-Topper. Fatigue & Fracture of Engineering Materials & Structures, 34, 854-867.

Kenmeugne, B., Soh Fotsing, B. D., Anago, G. F., Fogue, M., Robert, J. L., & Kenne. J. P. (2012). On the evolution and comparison of multiaxial fatigue criteria. International Journal of Engineering and Technology, 4, 37-46.

Kim, K., Geringer, J., Pellier, J., & Macdonald, D.D. (2013). Fretting corrosion damage of total hip prosthesis: Friction coefficient and damage rate constant approach. Tribology International, 60, 10–18.

Landolt, S., & Mischler, D. (2011). Tribocorrosion of passive metals and coatings. Woodhead Publishing Limited.

Luo, J., Cai, Z. B., Mo, J. L., Peng, J. F., & Zhu, M. H. (2016). Friction and wear properties of high-velocity oxygen fuel sprayed WC-17Co coating under rotational fretting conditions. Chinese Journal of Mechanical Engineering, 29, 515–521.

Lykins, C. D, Mall, S., & Jain, V. K. (2001). Combined experimental–numerical investigation of fretting crack initiation. International Journal of Fatigue, 23, 703–711.

Madge, J. J., Leen, S. B., & Shipway, P. H. (2007). The critical role of fretting wear in the analysis of fretting fatigue. Wear, 263, 542–551.

Magaziner, R. S., Jain, V. K., & Mall S. (2008). Wear characterization of Ti-6Al-4V under fretting – reciprocating sliding conditions. Wear, 264, 1002-1014.

Mezlini, S., Kapsa, Ph., Abry, J. C., & Guillemenet, J. (2006). Effect of indenter geometry and relationship between abrasive wear and hardness in early stage of repetitive sliding. Wear, 260, 412-421.

Pellinghelli, D., Riboli, M., & Spagnoli, A. (2018). Full model multiaxial fatigue life calculations with different criteria. Procedia Engineering, 213, 126–136.

Proudhon, H., Fouvry, S., & Buffiere, J. Y. (2005). A fretting crack initiation prediction taking into account the surface roughness and the crack nucleation process volume. International Journal of Fatigue, 27, 569–579.

Salerno, G., Magnabosco, R., & de Moura Neto, C. (2007). Mean strain influence in low cycle fatigue behaviour of AA7175-T1 aluminum alloy. International Journal of Fatigue, 29, 829–835.

Shen, M. X., Cai, Z. B., Mo, J. L., & Zhu, M. H. (2015). Local fatigue and wear behaviours of 7075 aluminium alloy induced by rotational fretting wear. International Journal of Surface Science and Engineering, 9, 520-537.

Shen, M. X., Cai, Z. B., Peng, J. F., Peng, X. D., & Zhu, M. H. (2016). Antiwear properties of bonded MoS2 solid lubricant coating under dual-rotary fretting conditions. Tribology Transactions, 60, 217-225.

Shen, M. X., Zhou, Y., Song, C., Mo, J. L., Cai, Z. B., & Zhu, M. H. (2013). Local fatigue behavior of 7075 alloy under condition of rotational fretting wear. Journal of Aeronautical Materials, 33, 46-50.

Szolwinsky, M. P., & Farris, T.N. (1998). Observations, analysis and prediction of fretting fatigue in 2024-T351 aluminium alloy. Wear, 221, 24–36.

van Lieshout, P. S., den Besten, J. H., & Kaminski, M. L. (2017). Validation of the corrected Dang Van multiaxial fatigue criterion applied to turret bearings of FPSO offloading buoys. Ships and Offshore Structures, 12, 521-529.

Williams, J. A., & Dwyer-Joyce, R. S. (2001). Contact between solid surfaces. In Modern tribology handbook, ed. Bharat Bhushan, volume one – Principles of tribology. CRC Press LLC, chapter 3.
Yang, J., Mo, J. L., Cai, Z. B., Xiao, X. B., & Zhu, M. H. (2013). Identification between rotational fretting and rotational wear of PMMA/steel by means of tribo-noise and tribo-vibration signals. Tribology International, 59, 1–9.
Zheng, J. F., Yang, S., Shen, M. X., Mo, J. L., & Zhu, M. H. (2011). Study on rotational fretting wear under a ball-on-concave contact configuration. Wear, 271, 1552-1562.
Zhou, Y., Shen, M. X., Cai, Z. B., & Zhu, M. H. (2017). Study on dual rotary fretting wear behavior of Ti6Al4V titanium alloy. Wear 376-377, 670-679.